Nanocatalysis

Deutsche Ausgabe: DOI: 10.1002/ange.201511764
Internationale Ausgabe: DOI: 10.1002/anie.201511764

Nanoplasmonic Photoluminescence Spectroscopy at Single-Particle Level: Sensing for Ethanol Oxidation

*Zhaoke Zheng and Tetsuro Majima**

Abstract: *Surface plasmon resonances of metal nanoparticles have shown significant promise for the use of solar energy to drive catalytic chemical reactions. More importantly, understanding and monitoring such catalytic reactions at single-nanoparticle level is crucial for the study of local reaction processes. Herein, using plasmonic photoluminescence (PL) spectroscopy, we describe a novel sensing method for catalytic ethanol oxidation reactions at the single-nanoparticle level. The Au nanorod monitors the interfacial interaction with ethanol during the catalytic reaction through the PL intensity changes in the single-particle PL spectra. The analysis of energy relaxation of excited electron–hole pairs indicates the relationship between the PL quenching and ethanol oxidation reaction on the single Au nanorod.*

Plasmonic metal nanoparticles (NPs) have been widely used to improve the efficiency of photocatalysis,[1] photovoltaics,[2] and photodetectors,[3] either by increasing light absorption through enhanced local fields[4] or by plasmon-induced charge transfer process.[5] Surface plasmon resonance (SPR) is described as the resonant photo-induced collective oscillation of conduction electrons. After light absorption and SPR excitation, plasmons can decay radiatively through re-emitted photons or non-radiatively by formation of hot electrons.[2a] The hot electron, generated either by plasmon decay or interband excitations, can induce photochemical transformations either through localized heating of the nanostructures or by energetic charge transfer to the reactants adsorbed on the surface of the NPs.[6] Therefore, another promising use of plasmonic nanostructures centers on recently demonstrated direct SPR-induced photocatalysis on excited plasmonic metal NPs.[7]

Meanwhile, to monitor the chemical reaction on single-metal NPs, nanoplasmonic sensing strategies have been adapted and tailored successfully for probing catalysts in situ and in real time.[8] One of the strategies relies on the SPR sensitivity towards the changes of the plasmonic particles itself, since the SPR frequency of metallic NPs is well-known to depend strongly on the particle size, shape and materials. Another strategy relies on significant sensitivity of SPR towards changes in the plasmonic NPs environment via the enhanced field, including direct nanoplasmonic sensing[9] and indirect nanoplasmonic sensing.[10] In these strategies, the wavelength of maximum light extinction of SPR, λ_{max}, is used as the main observable and its shift provides the main sensing function. One of the main weaknesses is that the readout simply corresponds to spectra shift of the SPR, while the absorbance intensity at λ_{max} did not change greatly during the sensing measurement. Recently, we found that the photoluminescence (PL) of single excited Au nanorod (NR) is sensitive to the surroundings when charge transfer occurred.[11] Thus, the plasmonic PL can be a promising sensing probe for the local chemical reactions.

Early efforts to understand the PL from gold NPs have relied on ensemble measurements. By measuring the photoemission from ensembles of gold nanospheres, Wilcoxon et al. assigned the PL to the radiative recombination of Fermi level electrons and sp- or d-band holes created after photoexcitation.[12] Mohammed et al.[13] have measured the PL from ensembles of gold nanorods (NRs) and only one peak appeared in the emission spectra. The observed PL was explained by the radiative recombination of electron-hole pairs that is enhanced by local fields associated with the SPR. However, the ensemble measurements are inaccurate because of the presence of inhomogeneities within the sample, and the signal can be easily influenced because of a small number of aggregates of NPs. Single-particle measurements are essential to exclude undesirable effects from ensemble studies and better understand the PL mechanism. With this technique, plasmonic PL from individual Au NRs has been studied by Link and co-wordkers.[14] They found that the PL spectrum closely reproduces the shape of the scattering spectrum and assigned the PL to the radiative decay of surface plasmons. By collecting the PL spectrum of a single Au NR with 785 nm excitation, they excluded that interband transitions are the cause of the PL. Such a PL mechanism of single Au NR was also confirmed and elucidated by Wackenhut et al.[15]

After understanding the intrinsical physics of PL in single Au NRs, the PL spectroscopy can be explored as a direct nanoplasmonic probe of local catalytic reactions on excited Au NRs. Herein, we describe a sensing method for plasmon-induced ethanol oxidation reactions at the single-particle level by using plasmonic PL spectroscopy. Ethanol oxidation is a common model reaction relevant for photocatalytic H_2 production, since ethanol is widely used as an efficient electron donor. This work can help us to better understand the interaction between ethanol and photo-excited Au NPs in direct SPR-induced photocatalysis as well as in the system of plasmonic photocatalyst, for example, Au-TiO_2.

Our strategy is shown in Figure 1. We synthesized Au NRs by the seed-mediated method.[16] Figure 1a shows a transmission electron microscopy (TEM) image and an extinction

[*] Dr. Z. Zheng, Prof. Dr. T. Majima
The Institute of Scientific and Industrial Research (SANKEN)
Osaka University, Mihogaoka 8-1, Ibaraki, Osaka 567-0047 (Japan)
E-mail: majima@sanken.osaka-u.ac.jp

Supporting information for this article is available on the WWW under http://dx.doi.org/10.1002/anie.201511764.

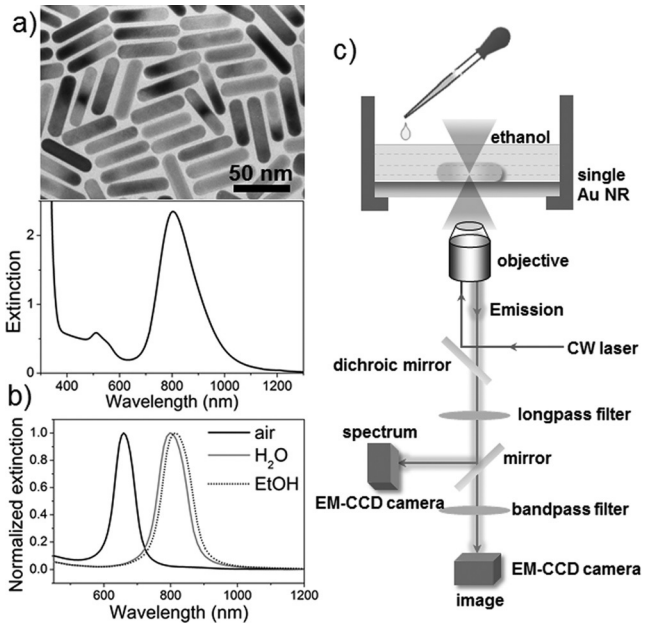

Figure 1. a) TEM image and UV/Vis/NIR extinction spectra of the as-prepared Au NRs. b) Calculated extinction spectrum at the LSPR region for Au NRs immersed in various surroundings using the FDTD method. c) Illustration of single-particle PL measurement based on confocal microscope system.

spectrum of the as-synthesized Au NRs. These NRs have an average aspect ratio of 3.9, and they gave rise to a longitudinal surface plasmon resonance (LSPR) peak centered at about 804 nm. The extinction spectrum was obtained from the sample dispersed in water solutions. The confocal microscope system with a special sample cell was used to directly monitor the PL behavior of single Au NRs interacting with ethanol (Figure 1 c). Firstly, mono-dispersed Au NRs in low concentration (0.016 mg mL^{-1}) were spin-coated on the pre-cleaned quartz cover glass, which was subsequently annealed at 100 °C for 30 minutes to immobilize the Au NRs on the quartz glass. Then the immobilized sample was treated with O_3 for 15 minutes to remove the residual surfactant on the Au NRs. The single-particle PL measurement was carried out with a circular-polarized 405 nm continuous-wave (CW) laser, while the interband transition of Au NRs was excited. For the PL measurement, suitable dichroic mirror and long pass filters were used to completely remove the laser excitation light. The PL image was obtained by a single-photon avalanche diode (SPAD). While for the spectroscopy, the emission passed through a slit with a width of 150 μm and was collected by an electron-multiplying charge-coupled device (EMCCD) camera. Meixner et al. reported that the PL from Au nanostructures can also be enhanced by an applied bias voltage,[17] which could potentially further increase the sensitivity of this method when performed in an electrochemical cell.

Since the absorbance of the sample that dispersed on quartz glass is very weak because of the low concentration, it was difficult to directly measure the extinction spectra by the experimental method. We thus carried out the finite difference time domain (FDTD) calculations on Au NRs that immersed in various surroundings. As shown in Figure 1 b, the LSPR peak of the sample that immersed in water centered at 801 nm, which is in agreement with experimental results obtained from the as-prepared Au NR suspensions (Figure 1 a). When immersed in ethanol, the LSPR peak in the calculated extinction spectra exhibits a slight red shift to 815 nm, which is due to the relatively larger refractive index of ethanol (ca. 1.36) compared with that of water (ca. 1.33). The sample that exposed to air shows a LSPR peak position at 659 nm considering that the refractive index of air is about 1.

As a reference, the PL of the single Au NR was first measured without ethanol, means, the Au NR was exposed to ambient air. Then the PL from the same Au NR immersed in ethanol was obtained by gently filling the cell with ethanol. The information of interfacial interaction between excited Au NRs and ethanol can be analyzed by monitoring the PL changes. The principle here is somewhat different with the currently intensely explored nanoplasmonic probes, which based on the λ_{max}-shift of single Au NPs in dark field scattering spectra. In our case, the PL from Au NRs has a close relationship with the excited electron-hole pairs, which are essential for the catalytic reactions on the plasmonic NPs. Thus, using the plasmonic PL as the direct probe can help us to analysis the reaction process occurred simultaneously.

Figure 2 a shows a typical single-particle PL image of Au NRs exposed to ambient air. To confirm that the PL bright dots are coming from individual Au NRs, the mono-dispersibility of the sample was investigated. Figure S1 in the Supporting Information shows typical SEM images of mono-dispersed Au NRs on a quartz cover glass substrate, which confirms the mono-dispersibility of our sample. The PL image

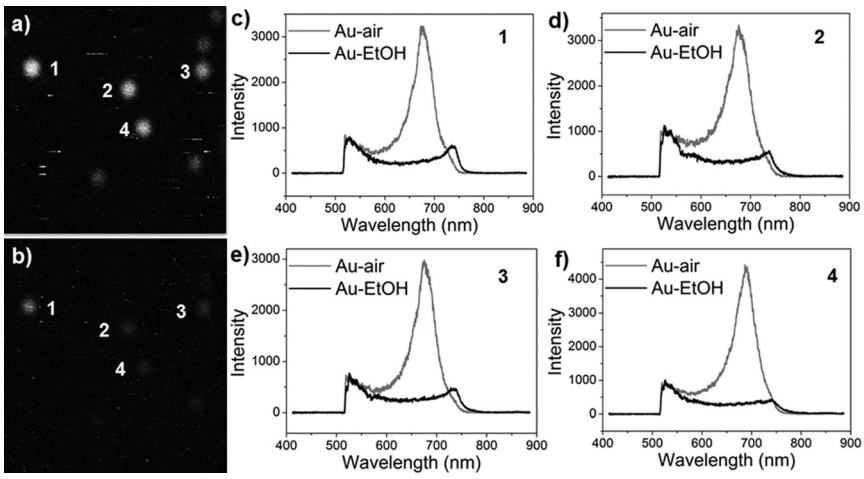

Figure 2. a–b) PL images of single Au NRs dispersed on quartz cover glass: a) exposed to ambient air and b) immersed in ethanol. c–f) PL spectra of the corresponding single Au NRs as numbered in the PL images. The grey and black lines represent the PL spectra from the same Au NR exposed to air and immersed in ethanol, respectively.

of the same Au NRs immersed in ethanol was obtained by the same way except filling the cell with ethanol (Figure 2b). It can be found that the PL intensities of Au NRs decreased when they were immersed in ethanol. The PL spectra of the corresponding single Au NRs as numbered in the PL image are shown in Figure 2c–f. A strong PL peak at the LSPR region was observed for Au NRs exposed to air. Since a long pass filter ($\lambda > 513$ nm) was installed to remove the excitation light, the PL at the transversal surface plasmon resonance (TSPR) region was not fully displayed. When the same Au NRs were immersed in ethanol, the PL intensities at the LSPR region dramatically decreased compared with those exposed to air. Meanwhile, there is a conspicuous red-shift of the LSPR PL peak, which is consistent with the extinction spectra calculated by FDTD method shown in Figure 1b.

The LSPR PL maximum and intensities of single Au NRs are sensitive to the aspect ratio and diameters,[11a,18] thus to study the same single Au NRs immersed in various surroundings is very essential to exclude undesirable effects caused by sample heterogeneity. Here, we can obtain the in situ characterization on the same Au NRs to directly observe the PL quenching effect and hence study the interaction between Au NRs and ethanol. The obvious decrease of the LSPR PL intensities indicates that the PL in the LSPR mode was quenched by the surrounding ethanol.

To further verify that the quenching phenomenon of ethanol-surrounded Au NRs is not steming from the coating effect, the single-particle PL of Au NRs immersed in water were also measured (Figure 3). The PL images of single Au NRs exposed to ambient air and immersed in H_2O show similar PL intensities. The PL spectra of the corresponding single Au NRs as numbered in Figure 3a–b were compared in Figure 3c–f. Only a red-shift of the LSPR maximum was observed in the PL spectra for the sample immersed in water, which is consistent with the extinction spectra calculations shown in Figure 1b; while there is no obvious change in the intensities of LSPR PL. Therefore, the PL of Au NRs can be quenched by surrounding ethanol but not by water in the same exciting conditions.

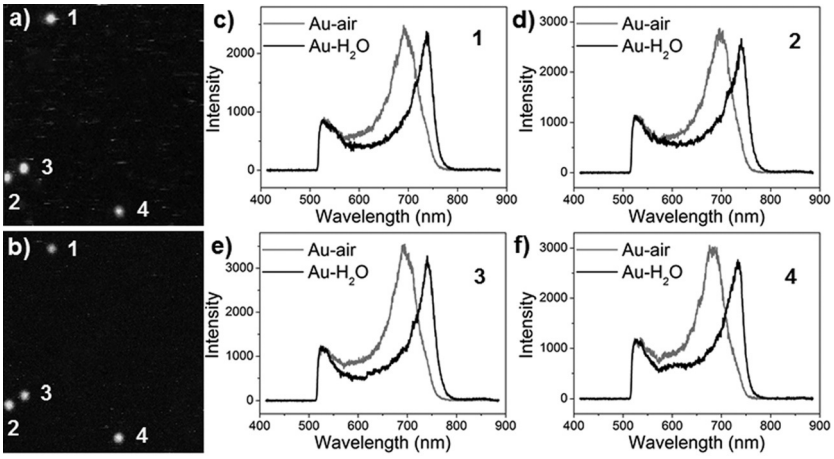

Figure 3. a–b) PL images of single Au NRs dispersed on quartz cover glass: a) exposed to ambient air and b) immersed in H_2O. c–f) PL spectra of the corresponding single Au NRs as numbered in the PL images.

In our single-particle PL measurement, a circular-polarized 405 nm CW laser was used as the light source. In this case, only the interband transition of Au NRs was excited while neither TSPR mode nor LSPR mode was directly excited. The interband transition created electron–hole pairs, which can relax very efficiently through a fast interconversion in the TSPR mode and subsequently decay radiatively to generate the TSPR PL. Meanwhile, the electron-hole pairs lose their energy and interconvert to the LSPR mode, which can radiatively decay to generate the LSPR PL. This PL mechanism is consistent with the reported works.[14b,15] While the radiative recombination of electron-hole pairs cannot well explain the PL of single Au NR since both TSPR and LSPR mode are observed in the PL spectra.

Normally only the longitudinal mode of PL can be greatly influenced by the aspect ratio (Figure S4) and local environment, while the transverse mode is almost unaffected. To study the different influence of hot electron transfer on the transverse and longitudinal modes, we investigated the PL behaviour of Pt-modified Au NRs, in which the hot electron can transfer from Au NRs to Pt because of the higher work function of Pt.[11a] As shown in Figure S5, compared with Au NRs, the Pt-modified Au NRs show dramatically decrease for the LSPR PL intensity, which is assigned to the electron transfer process, while the transverse mode is almost uninfluenced. It indicates that electron transfer does not equally affect the transverse and longitudinal modes. Furthermore, compared with the emission from the TSPR mode (ca. 5 fs), the emission linked to the LSPR mode has a relatively longer lifetime ranging from 9 to 18 fs.[15] It indicates that the LSPR PL is easier to be influenced for the occurrence of interfacial interactions. Thus, the LSPR PL can be explored as a direct nanoplasmonic probe for local catalytic reactions on excited Au NPs.

It has been evidenced that various alcohols can be oxidized by plasmonic Au NPs under visible light irradiation.[19] In the field of photocatalytic water splitting, ethanol is an efficient and widely used electron donor. Tian et al also confirmed that the plasmonic Au NPs can oxidize ethanol at the expense of oxygen reduction under visible light.[20] In our case, when Au NRs were immersed in ethanol, the hot electrons can transfer from the excited Au NRs to dissolved oxygen, while the electron-deficient Au NRs can oxidize ethanol, which means that the excited charges are separated (Figure 4). Such a charge separation (CS) state will complete with the LSPR emission (Figure 4a), and hence give rise to the PL quenching at the LSPR region. Thus, the PL quenching phenomenon is closely related to the photocatalytic ethanol oxidation process, and hence the local ethanol oxidation reaction can be monitored by the changes of LSPR PL. When Au NRs was immersed in water, the hot electrons can still transfer to

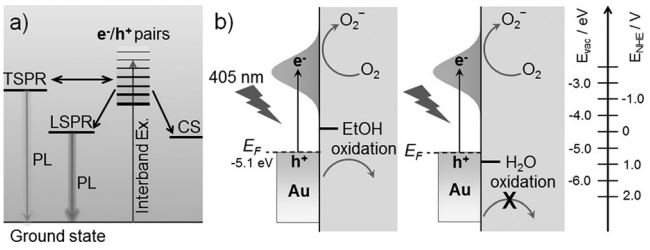

Figure 4. Schematic diagram of a) the mechanism for radiative decay of surface plasmon and b) interfacial charge transfer between excited Au NR and surroundings. The charge separation state CS and the Fermi energy E_F.

dissolved oxygen, however, the water cannot be oxidized by the electron-deficient Au, because the oxidation potential of water (0.817 eV vs. NHE, pH 7)[21] is much more positive than that of ethanol[22] (−0.197 V vs. NHE, pH 7). Thus the electron-hole pairs cannot be consumed simultaneously and hence the PL at the LSPR region was not quenched. Similar to that of photocatalytic process, half reactions cannot continue without electron or hole scavenger, since the accumulative electrons or holes will inhibit the half reactions. Such a sensing method will be further explored to study the oxygen-free condition as well as the interaction with other toxic solvent, once a suitable enclosed-sample-cell is developed in the future.

To further confirm that the excited Au NRs can facilitate ethanol oxidation at the expense of oxygen reduction under visible light, we carried out two-cell photo-electrochemical measurement (Figure S6a). The Au NRs were dispersed on carbon fibre (CF) anode, where ethanol oxidation reaction (EOR) occurred. Meanwhile, with light irradiation, the hot electrons can transfer to the Pt cathode for the oxygen reduction reaction (ORR). Figure S6b shows the cyclic voltammograms (CV) of the Au NRs for EOR in 0.1 M NaOH with 0.5 M ethanol electrolyte. With light irradiation, the EOR current was about three times compared with that in the dark, indicating that the electron-deficient Au NRs can efficiently facilitate ethanol oxidation under light irradiation. This is consistent with Tian's results that Au NPs can oxidize ethanol at the expense of oxygen reduction under visible light.[20] Without ethanol or without Au NRs, no anodic oxidation peak occurred.

The ORR measurements were also carried out to investigate the electron transfer process from Au to dissolved O_2. Figure S7a shows the rotating disk electrode (RDE) curves of Au NRs recorded at room temperature with varying rotating speed from 400 to 2000 rpm. The potential was scanned from −0.3 to +1.1 V versus reversible hydrogen electrode (RHE) at a scan rate of 10 mV s^{-1}. With an increase in the electrode rotation speed, the ORR diffusion-limiting current density gradually increases, indicating a prominent ORR catalytic activity. Figure S7b compared the ORR polarization curves with and without light irradiation at a rotation rate of 1600 rpm. Under light irradiation, the Au-NRs catalyst exhibited a higher diffusion-limiting current density than that in the dark. Additionally, the half-wave potential ($E_{1/2}$) of the catalyst under light irradiation is 0.80 V vs. RHE, which is more positive than that in the dark (0.77 V vs. RHE), indicating that the hot electrons on Au NRs can efficiently transfer to the dissolved O_2 under light irradiation.

To gain insight into the ORR pathways of the catalysts, the rotating ring-disk electrode (RRDE) results are shown in Figure S8 where the selectivity for four-electron reduction of oxygen is given in terms of hydrogen peroxide ion (HO_2^-). As a reference, commercial Pt/C catalyst was measured in the same conditions (Figure S8a). As shown in Figure S8b, the $E_{1/2}$ of Au NRs is only 80 mV negative shift compared with that of Pt/C (0.85 V vs. RHE). The average electron transfer number (n) for Au NRs catalyst was ≈3.9 (Figure S8c) and the yield of produced HO_2^- was less than 5% (Figure S8d), which are comparable to that of Pt/C, suggesting a dominant four-electron oxygen reduction process. The overall four-electron ORR also indicates an efficient electron transfer from Au NRs dissolved O_2.

The excited surface plasmons can also decay by the plasmon resonance energy transfer (PRET) process, namely, the interaction of neighbouring molecules with the SPR-induced electric-field amplification localized nearby at the Au NRs. To ascertain its possible contribution to the quenching of PL spectra, 3D FDTD simulation was performed to calculate the spatial distribution of electric field intensity (Figure S9). Surprisingly, the Au NRs exposed to air shows the highest amplification of local electric field while the sample immersed in ethanol exhibit the lowest enhancement. This indicates that ethanol has the weakest interaction with plasmonic Au NRs via the PRET process. Furthermore, due to the weak light absorption of water and ethanol in the visible region, the PRET process is not the reason for the PL quenching of Au NRs.

In conclusion, we developed a novel sensing method for monitoring of ethanol oxidation reactions at the single-nanoparticle level by using plasmonic PL spectroscopy. The catalytic ethanol oxidation reactions occurred on the surface of single Au NR results in an obvious quenching phenomenon for the PL of the same Au NR. The analysis of energy relaxation of excited electron-hole pairs indicates the relationship between PL quenching and ethanol oxidation reaction. FDTD simulations also indicate that the PRET process is not the reason for the PL quenching. Since the PL at the LSPR region is sensitive to the interfacial catalytic reactions of Au NRs, it can be employed as an efficient nanoplasmonic probe for the local catalytic reactions. Our sensing method may open a new field for nanoplasmonic sensing by monitoring the single-particle PL spectra other than the scattering spectrum, and the readout that contains both peak shift and intensity change could provide more information for the local changes.

Acknowledgements

This work has been supported by Innovative Project for Advanced Instruments, Renovation Center of Instruments for Science Education and Technology, Osaka University, and a Grant-in-Aid for Scientific Research (grant number 25220806) from the Ministry of Education, Culture, Sports,

Science and Technology (MEXT) of the Japanese Government. Z.Z. thanks the JSPS for a Postdoctoral Fellowship for Foreign Researchers (grant number P13027).

Keywords: gold nanorods · nanoparticles · plasmonic sensing · single-particle spectroscopy · surface plasmon resonances

How to cite: *Angew. Chem. Int. Ed.* **2016**, *55*, 2879–2883
Angew. Chem. **2016**, *128*, 2929–2933

[1] a) K. Wu, J. Chen, J. R. McBride, T. Lian, *Science* **2015**, *349*, 632–635; b) A. Marimuthu, J. Zhang, S. Linic, *Science* **2013**, *339*, 1590–1593.
[2] a) C. Clavero, *Nat. Photonics* **2014**, *8*, 95–103; b) S. Linic, P. Christopher, D. B. Ingram, *Nat. Mater.* **2011**, *10*, 911–921.
[3] a) M. W. Knight, H. Sobhani, P. Nordlander, N. J. Halas, *Science* **2011**, *332*, 702–704; b) M. L. Brongersma, N. J. Halas, P. Nordlander, *Nat. Nanotechnol.* **2015**, *10*, 25–34.
[4] J. A. Schuller, E. S. Barnard, W. Cai, Y. C. Jun, J. S. White, M. L. Brongersma, *Nat. Mater.* **2010**, *9*, 193–204.
[5] J. Li, S. K. Cushing, P. Zheng, T. Senty, F. Meng, A. D. Bristow, A. Manivannan, N. Wu, *J. Am. Chem. Soc.* **2014**, *136*, 8438–8449.
[6] S. Linic, U. Aslam, C. Boerigter, M. Morabito, *Nat. Mater.* **2015**, *14*, 744–744.
[7] a) P. Christopher, H. L. Xin, S. Linic, *Nat. Chem.* **2011**, *3*, 467–472; b) Q. Xiao, E. Jaatinen, H. Y. Zhu, *Chem. Asian J.* **2014**, *9*, 3046–3064.
[8] E. M. Larsson, S. Syrenova, C. Langhammer, *Nanophotonics* **2012**, *1*, 249–266.
[9] a) C. Novo, A. M. Funston, P. Mulvaney, *Nat. Nanotechnol.* **2008**, *3*, 598–602; b) L. Shi, C. Jing, W. Ma, D. W. Li, J. E. Halls, F. Marken, Y. T. Long, *Angew. Chem. Int. Ed.* **2013**, *52*, 6011–6014; *Angew. Chem.* **2013**, *125*, 6127–6130.
[10] a) C. Langhammer, E. M. Larsson, B. Kasemo, I. Zoric, *Nano Lett.* **2010**, *10*, 3529–3538; b) E. M. Larsson, C. Langhammer, I. Zoric, B. Kasemo, *Science* **2009**, *326*, 1091–1094.
[11] a) Z. K. Zheng, T. Tachikawa, T. Majima, *J. Am. Chem. Soc.* **2014**, *136*, 6870–6873; b) Z. K. Zheng, T. Tachikawa, T. Majima, *J. Am. Chem. Soc.* **2015**, *137*, 948–957.
[12] J. P. Wilcoxon, J. E. Martin, F. Parsapour, B. Wiedenman, D. F. Kelley, *J. Chem. Phys.* **1998**, *108*, 9137–9143.
[13] M. B. Mohamed, V. Volkov, S. Link, M. A. El-Sayed, *Chem. Phys. Lett.* **2000**, *317*, 517–523.
[14] a) A. Tcherniak, S. Dominguez-Medina, W.-S. Chang, P. Swanglap, L. S. Slaughter, C. F. Landes, S. Link, *J. Phys. Chem. C* **2011**, *115*, 15938–15949; b) Y. Fang, W.-S. Chang, B. Willingham, P. Swanglap, S. Dominguez-Medina, S. Link, *ACS Nano* **2012**, *6*, 7177–7184.
[15] F. Wackenhut, A. V. Failla, A. J. Meixner, *J. Phys. Chem. C* **2013**, *117*, 17870–17877.
[16] a) N. R. Jana, L. Gearheart, C. J. Murphy, *Adv. Mater.* **2001**, *13*, 1389–1393; b) B. Nikoobakht, M. A. El-Sayed, *Chem. Mater.* **2003**, *15*, 1957–1962.
[17] a) X. Wang, K. Braun, D. Zhang, H. Peisert, H. Adler, T. Chasse, A. J. Meixner, *ACS Nano* **2015**, *9*, 8176–8183; b) K. Braun, X. Wang, A. M. Kern, H. Adler, H. Peisert, T. Chasse, D. Zhang, A. J. Meixner, *Beilstein J. Nanotechnol.* **2015**, *6*, 1100–1106.
[18] M. Yorulmaz, S. Khatua, P. Zijlstra, A. Gaiduk, M. Orrit, *Nano Lett.* **2012**, *12*, 4385–4391.
[19] a) C. L. Wang, D. Astruc, *Chem. Soc. Rev.* **2014**, *43*, 7188–7216; b) R. Sellappan, M. G. Nielsen, F. Gonzalez-Posada, P. C. K. Vesborg, I. Chorkendorff, D. Chakarov, *J. Catal.* **2013**, *307*, 214–221.
[20] Y. Tian, T. Tatsuma, *J. Am. Chem. Soc.* **2005**, *127*, 7632–7637.
[21] Y. Xu, M. A. A. Schoonen, *Am. Mineral.* **2000**, *85*, 543–556.
[22] T. Simon, N. Bouchonville, M. J. Berr, A. Vaneski, A. Adrovic, D. Volbers, R. Wyrwich, M. Doblinger, A. S. Susha, A. L. Rogach, F. Jackel, J. K. Stolarczyk, J. Feldmann, *Nat. Mater.* **2014**, *13*, 1013–1018.

Received: December 19, 2015
Published online: January 25, 2016

